ELectronics EXpress

LETTER

IEICE Electronics Express, Vol.10, No.17, 1–9

Silicon Mach–Zehnder modulator using low-loss phase shifter with bottom PN junction formed by restricted-depth doping

Kazuhiro Goi[1a)], **Kensuke Ogawa**[1], **Yong Tsong Tan**[2], **Vivek Dixit**[3], **Soon Thor Lim**[3], **Ching Eng Png**[3], **Tsung-Yang Liow**[4], **Xiaoguang Tu**[4], **Guo-Qiang Lo**[4], **and Dim-Lee Kwong**[4]

[1] *Optics and Electronics Laboratory, Fujikura Ltd., 1440 Mutsuzaki, Sakura, Chiba 285–8550, Japan*

[2] *Power and Telecommunication Systems Company, Fujikura Ltd., 1440 Mutsuzaki, Sakura, Chiba 285–8550, Japan*

[3] *Institute of High Performance Computing, Agency for Science, Technology and Research (A*STAR), 1 Fusionopolis Way, #16–16 Connexis, Singapore 138632, Singapore*

[4] *Institute of Microelectronics, Agency for Science, Technology and Research (A*STAR), 11 Science Park Road, Singapore Science Park II, Singapore 117685, Singapore*

a) *kazuhiro.goi@jp.fujikura.com*

Abstract: A silicon Mach–Zehnder modulator with a low-loss phase shifter formed by restricted-depth doping is fabricated and characterized. The phase shifter has a PN junction at the bottom of the rib waveguide, whereas the top of the rib is un-doped. Device simulations confirm that the phase-shifter loss is reduced by 26 − 28% with an increased phase-shifter length to keep a π phase shift with the same bias condition in comparison with a conventional PN junction through the whole depth. An optical loss as low as 1.6 dB has been achieved in the fabricated phase shifter with a 6-mm length. The Mach–Zehnder modulator with the phase shifter has a fiber-to-fiber loss of 9 dB. 10-Gbps non-return-to-zero on-off keying with extinction ratio of 11 dB is demonstrated under push-pull operation with a 6 V_{pp} driving voltage on each arm.

Keywords: modulators, waveguide modulators, silicon photonics

Classification: Optoelectronics, Lasers and quantum electronics, Ultrafast optics, Silicon photonics, Planar lightwave circuits

References

[1] E. L. Wooten, K. M. Kissa, A. Yi-Yan, E. J. Murphy, D. A. Lafaw, P. F. Hallemeier, D. Maack, D. V. Attanasio, D. J. Fritz, G. J. McBrien and D. E. Bossi: IEEE J. Sel. Topics Quantum Electron. **6** (2000) 69.

[2] L. Liao, A. Liu, D. Rubin, J. Basak, Y. Chetrit, H. Nguyen, R. Cohen, N. Izhaky and M. Paniccia: Electron. Lett. **43** (2007) 1196.

DOI: 10.1587/elex.10.20130552
Received July 15, 2013
Accepted August 02, 2013
Publicized August 15, 2013
Copyedited September 10, 2013

[3] D. J. Thomson, F. Y. Gardes, Y. Hu, G. Mashanovich, M. Fournier, P. Grosse, J.-M. Fedeli and G. T. Reed: Opt. Express **19** (2011) 11507.
[4] P. Dong, L. Chen and Y.-K. Chen: Opt. Express **20** (2012) 6163.
[5] X. Xiao, H. Xu, X. Li, Z. Li, T. Chu, Y. Yu and J. Yu: Opt. Express **21** (2013) 4116.
[6] M. Ziebell, D. Marris-Morini, G. Rasigade, J.-M. Fédéli, P. Crozat, E. Cassan, D. Bouville and L. Vivien: Opt. Express **20** (2012) 10591.
[7] X. Tu, T.-Y. Liow, J. Song, X. Luo, Q. Fang, M. Yu and G.-Q. Lo: Opt. Express **21** (2013) 12776.
[8] K. Ogawa, K. Goi, Y. T. Tan, T.-Y. Liow, X. Tu, Q. Fang, G.-Q. Lo and D.-L. Kwong: Opt. Express **19** (2011) B26.
[9] K. Goi, K. Oda, H. Kusaka, Y. Terada, K. Ogawa, T.-Y. Liow, X. Tu, G.-Q. Lo and D.-L. Kwong: Opt. Express **20** (2012) B350.
[10] X. Tu, T.-Y. Liow, J. Song, M. Yu and G. Q. Lo: Opt. Express **19** (2011) 18029.
[11] R. A. Soref and B. R. Bennet: IEEE J. Quantum Electron. **23** (1987) 123.
[12] X. Tu, S. Chen, L. Zhao, F. Sun, J. Yu and Q. Wang: J. Lightwave Technol. **24** (2006) 1000.
[13] S. M. Sze and K. K. Ng: *Physics of Semiconductor Devices* (John Wiley & Sons, New Jersey, 2007) 3rd ed. 32.
[14] T.-Y. Liow, K.-W. Ang, Q. Fang, J.-F. Song, Y.-Z. Xiong, M.-B. Yu, G.-Q. Lo, and D.-L. Kwong: IEEE J. Sel. Topics Quantum Electron. **16** (2010) 307.
[15] Q. Fang, J. Song, X. Luo, M. Yu, G. Lo and Y. Liu: Opt. Express **19** (2011) 21588.
[16] K. Yamada, T. Tsuchizawa, T. Watanabe, J. Takahashi, E. Tamechika, M. Takahashi, S. Uchiyama, H. Fukuda, T. Shoji, S. Itabashi and H. Morita: IEICE Trans. Electron. **E87-C** (2004) 351.
[17] J. Shin, C. Ozturk, S. R. Sakamoto, Y. J. Chiu and N. Dagli: IEEE Trans. Microw. Theory Tech. **53** (2005) 636.
[18] S. Akiyama, H. Itoh, T. Takeuchi, A. Kuramata and T. Yamamoto: Electron. Lett. **41** (2005) 40.

1 Introduction

High-speed modulators are key components in optical communication systems. In particular, Mach–Zehnder modulators (MZMs) are widely used because they provide signal modulation without frequency chirping under push-pull operation. MZMs can thus suppress signal degradation caused by pulse and spectral broadening associated with chromatic dispersion in optical fibers for long-distance optical communications. The practical MZMs have been developed using lithium niobate (LN) [1]. They are widely used in current systems.

Increasing data traffic in the optical communication systems requires greater reduction in the cost and size of optical components. However, the cost reduction of the LN MZMs is limited because of their large footprint and small wafer size. Silicon modulators are capable of meeting these requirements due to features, such as their small footprint and low fabrication cost using well-developed complimentary metal-oxide-semicon-

DOI: 10.1587/elex.10.20130552
Received July 15, 2013
Accepted August 02, 2013
Publicized August 15, 2013
Copyedited September 10, 2013

ductor (CMOS) compatible technologies. Various types of silicon MZMs have therefore been widely studied. Some of them have even achieved 40-Gbps on-off-keying (OOK) by operating in carrier depletion mode [2, 3, 4, 5, 6, 7]. For long-distance optical communications, signal qualities such as extinction ratio (ER) and chirp characteristics are important. The silicon MZM with a reduced series resistance is able to provide a high ER over 10 dB at 10–12.5 Gbps [8] and achieved long-distance transmission up to 80 km [9]. For a modulator to see commercial use, it must have low insertion loss in addition to the high-quality signal. Recently, a low-loss silicon MZM using a lateral PN junction has been reported [5]. The high modulation efficiency was realized using strong optical confinement in the thick silicon waveguide of 340-nm height instead of 220-nm height widely used for silicon waveguide devices. Optimization of a dopant profiles in 220-nm height waveguides [10] and an improved PN junction design [6] are also reported respectively. The doping profiles are fabricated using complicated fabrication steps in comparison with the conventional PN junction.

In this paper, we report a low-loss silicon MZM with a bottom PN-junction phase shifter formed by restricted-depth doping. A simple process is used for the fabrication of a silicon modulator with a waveguide thickness of 220 nm. First, we introduce the design and show the results of simulations that demonstrate the effectiveness of the proposed structure in reducing the optical loss of the phase shifter. Second, we describe the fabrication of the modulator using simple CMOS-compatible processes. Optical-loss measurement of the modulator confirms that the proposed structure is low optical loss under DC operation. Finally, we demonstrate the high-speed operation of the fabricated MZM. The MZM has a low phase-shifter loss of 1.6 dB and operates at a 10-Gbps non-return-to-zero (NRZ) OOK with a 6 V_{pp} driving voltage on each arm.

2 Design and simulation

2.1 Phase shifter design

Fig. 1 (a) shows a schematic of the proposed silicon phase shifter. The rib waveguide contains the lateral PN junction. The doped region is restricted to the bottom of the rib, while the top of the rib is un-doped. Both sides of the PN junction are heavily doped to ensure ohmic contacts with the metal of the upper electrode and to reduce the series resistance between the PN junction and the contacts.

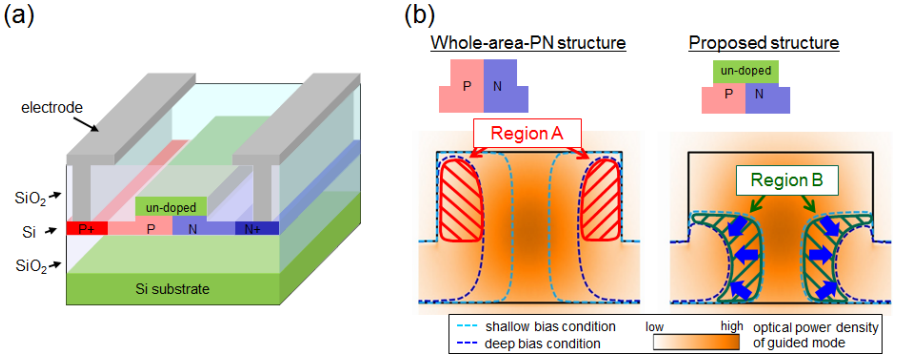

Fig. 1. (a) Schematic of the proposed phase shifter, and (b) carrier distributions under DC bias superimposed with the optical mode field.

DOI: 10.1587/elex.10.20130552
Received July 15, 2013
Accepted August 02, 2013
Publicized August 15, 2013
Copyedited September 10, 2013

Applying a bias voltage to the electrode changes the free carrier concentration at the PN junction. These free carriers induce a phase change and modulate the optical wave passing through the phase shifter. However, the optical wave also experiences the absorption due to the free carriers [11]. The phase-shifter loss $l_{carrier}$ can be represented by the expression:

$$l_{carrier} = \left(\kappa_{eff}/\Delta n_{eff}\right) \cdot \varphi_{req} \cdot 20\log_{10} e, \tag{1}$$

where κ_{eff} is the imaginary part of the effective refractive index, Δn_{eff} is the change of the real part of the effective refractive index caused by the change of the carrier concentration from changing applied bias, and φ_{req} is the required phase shift (for example, $\varphi_{req} = \pi$ for OOK modulation with single-arm drive using an MZM). Since κ_{eff} depends on the applied bias, we use κ_{eff} at the center of the applied bias range (for example, we use κ_{eff} at -5 V when the applied bias changes from -6 V to -4 V). The loss depends not only on κ_{eff}, but also on Δn_{eff}, because the device length needed to achieve a phase shift φ_{req} is determined by Δn_{eff}. Therefore, as Eq. (1) suggests, a decrease in κ_{eff} and an increase in Δn_{eff} are necessary to reduce the phase-shifter loss.

Here we explain the low optical loss of the proposed structure in terms of κ_{eff} and Δn_{eff}. Fig. 1 (b) illustrates the changes of carrier distributions in the two phase shifters. The structure shown in the left schematic, designated as "Whole-area-PN structure", has uniform doping throughout the entire rib. The right schematic shows the proposed structure, which has the doped region restricted to the bottom of the rib. In each schematic, the dotted lines indicate the border between the high carrier-concentration region and the depletion region. The light-blue lines are of shallow bias conditions and the dark-blue lines are of deep bias conditions. The orange-colored shadows show the optical power density of the guided mode. First, we consider κ_{eff}. As shown by the dark-blue dotted line in the schematic of the "Whole-area-PN structure," the depletion region does not spread to the edge of the rib in the deep bias condition. The carriers around the edge of the rib, such as those in the area marked "Region A," do not contribute to the phase shift but do increase κ_{eff}. In contrast, the region in the "Proposed structure" corresponding to "Region A" in the "Whole-area-PN structure" is left un-doped due to the restriction of the doped region. The proposed structure thereby provides a low κ_{eff}. Second, we consider effects on Δn_{eff}. "Region B" in the proposed structure indicates the change of the depletion region. The diagonal direction change of the depletion region is caused by confinement of the electric field to the small region, and hence the change becomes large. Moreover, Δn_{eff} is also enhanced by the high mode-field density around the depleted region. It seems that the restriction of the doped region also reduce Δn_{eff}; however, the reduction of Δn_{eff} in the proposed structure is suppressed for these reasons. Taking into account both of κ_{eff} and Δn_{eff}, the proposed structure can function as a low-loss phase shifter.

2.2 Electrical and optical device simulations

Electrical and optical device simulations confirm that the proposed structure can be used as a low-loss phase shifter. We calculated the effective refractive indices for different bias voltages using optical simula-

DOI: 10.1587/elex.10.20130552
Received July 15, 2013
Accepted August 02, 2013
Publicized August 15, 2013
Copyedited September 10, 2013

tions with carrier distribution profiles obtained from electrical simulations, using a previously reported method [12]. The inset of Fig. 2 (a) shows the simulated structure. The rib width w_R and the thickness of the center rib region t_R are 500 and 220 nm, respectively. The thickness of the slab on each side of the rib region t_S is 95 nm. We assumed an uniform doping concentration of 3×10^{17}, 4×10^{17} and $5\times10^{17}\,\mathrm{cm}^{-3}$ in each P and N region for simplicity. Bias was applied through the heavily doped ($1\times10^{20}\,\mathrm{cm}^{-3}$) regions, which are located 1.2 μm away from the center of the PN junction. We simulated structures with doped regions of varying thicknesses t_D of 95, 140, 180 or 220 nm. A device simulator by Silvaco was used for electrical simulations and an optical simulator by RSoft was used for optical simulations.

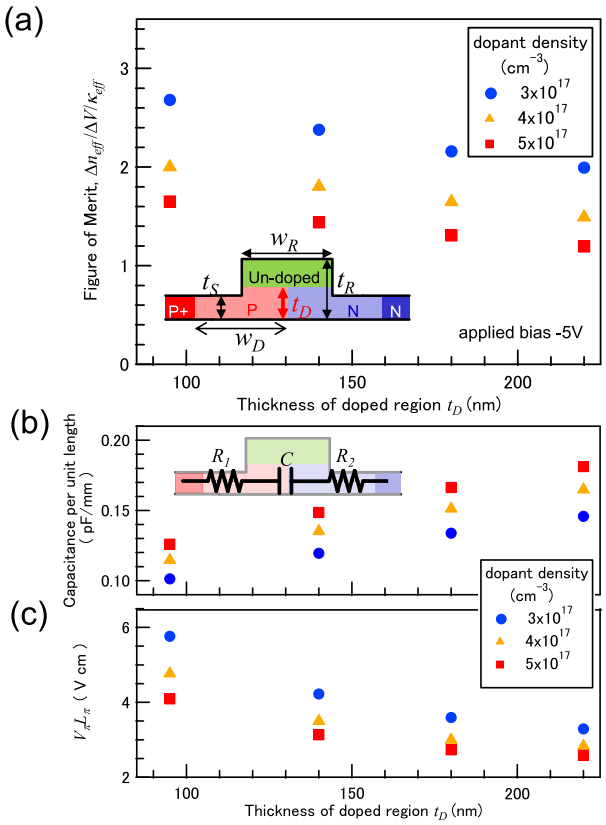

Fig. 2. (a) Figure of merit $\Delta n_{eff}/\Delta V/\kappa_{eff}$, (b) junction capacitance and (c) $V_\pi L_\pi$ simulated in each thickness of doped region.

Because changes in carrier concentration affect both κ_{eff} and Δn_{eff}, the voltage dependencies on both κ_{eff} and Δn_{eff} must be accounted for simultaneously to evaluate the efficiency of the phase shifter. Therefore, we introduce $(\Delta n_{eff}/\Delta V)/\kappa_{eff}$ as a figure of merit (FOM), which is inversely proportional to the optical loss caused by free carrier absorption described by Eq. (1).

Fig. 2 (a) shows the FOM versus the thickness of the doped region. Δn_{eff} at each applied bias V_{bias} is defined as the change in n_{eff} over the range of ΔV, such that: $\Delta n_{eff}(V_{bias}) = n_{eff}(V_{bias}+\Delta V/2) - n_{eff}(V_{bias}-\Delta V/2)$. Here $\Delta V = 1$ and $V_{bias} = -5$ V in Fig. 2. As Fig. 2 (a) shows, we find that structures with smaller t_D values have higher FOMs in each dopant densities. The structure with a

DOI: 10.1587/elex.10.20130552
Received July 15, 2013
Accepted August 02, 2013
Publicized August 15, 2013
Copyedited September 10, 2013

shallow doped region of t_D = 95 nm has 34 − 38% higher FOMs than that with t_D = 220 nm. This increased FOM corresponds to 26 − 28% lower phase-shifter losses. The structure with a smaller t_D can thus provides a lower-loss phase shifter.

Reducing the dopant density also increases the FOM of the phase shifter; however, doing so also deteriorates its high-speed performance. Because modulation under reverse bias is considered to be the depletion and accumulation of the carriers in the junction, the high-speed response of the phase shifter is limited by its resistor − capacitor coupling. The inset of Fig. 2 (b) shows the equivalent circuit model of the phase shifter, where R_1 and R_2 denote the series resistances in the slab regions, and C denotes the PN junction capacitance. The response time τ defined as $(R_1+R_2)C$ must be small for high-speed operation. Fig. 2 (b) shows the simulated junction capacitance per unit length. If the phase-shifter length becomes double, the capacitance becomes double and the resistance becomes half. Because the response time is thus not affected, the capacitance per unit length can be used for comparison. In the proposed structure, the junction capacitance is smaller than that in the whole-area-PN structure, while their resistances are the same; thus, τ is smaller in the proposed structure. The whole-area-PN structure with a low dopant density has a low junction capacitance, however, the series resistance is large because of the high resistivity of the slab region. For example, capacitance decreases by 20% when the dopant density changes from 5×10^{17} to 3×10^{17} cm^{-3}, while the resistivity increases by 30% (0.067 to 0.093 Ω·cm) for boron-doped silicon and 40% (0.033 to 0.043 Ω·cm) for phosphorus-doped silicon [13]. Thus, the restricted-depth doped phase shifter has better high-speed response than the whole-area-PN phase shifter with a low dopant density.

Fig. 2 (c) shows $V_\pi L_\pi$, which is frequently used to compare performance between modulators. The $V_\pi L_\pi$ values plotted in Fig. 2 (c) are calculated as $(\lambda/2)/(\Delta n_{eff}/\Delta V)$ from −4.5 to −5.5 V (ΔV =1). The $V_\pi L_\pi$ of the proposed structure is higher than that of the whole-area-PN structure. Thus, the proposed structure can be used as a low-loss phase shifter at the cost of being longer.

3 Experimental results and discussions

3.1 Fabrication of the proposed phase shifter

We fabricated the proposed bottom PN junction structure on a SOI wafer using CMOS-compatible processes, as shown in Fig. 3 (a). Before its top silicon layer is etched to form a rib waveguide, boron is implanted into the top silicon layer to form a P-type region. With high-energy implantation, boron atoms diffuse into the lower area of the top silicon layer. In the same manner, high-energy implantation of phosphorus forms the N-type region at the bottom of the top silicon layer and adjacent to the P-type region. After implantation for the P- and N-type regions, the rib structure is fabricated by dry etching. In this way, the PN junction is located near the bottom of the rib waveguide. Fig. 3 (b) shows the dopant distribution of the structure, calculated using a process simulator by Silvaco. The highly doped region is located at the bottom of the rib region, as expected.

The phase shifter has a slab thickness of 95 nm, a rib thickness of 220 nm, and a rib width of 500 nm. For comparison, we also fabricated a

DOI: 10.1587/elex.10.20130552
Received July 15, 2013
Accepted August 02, 2013
Publicized August 15, 2013
Copyedited September 10, 2013

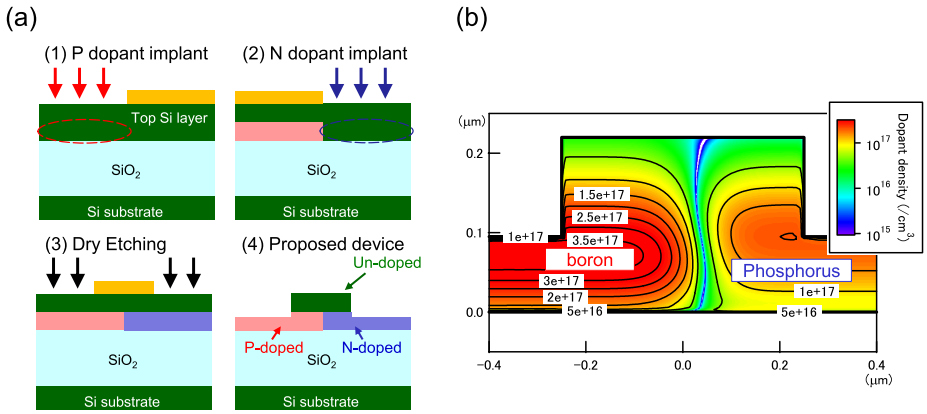

Fig. 3. (a) Fabrication processes of the proposed phase shifter and (b) expected dopant concentration by the proposed processes, which is calculated using a process simulator.

waveguide using the whole-area-PN structure [8, 14]. As mentioned in section 2.1, the whole-area-PN structure has a doped region from the top of the rib to the bottom and the same dimensions as the proposed structure.

3.2 Phase shifter characteristics

Here, we discuss the DC experimental results. The loss and phase shift of each fabricated phase shifter were measured in each bias condition. Fig. 4 (a) shows the transmission spectrum of an asymmetric MZ interferometer with phase shifter of 6-mm length. Changing the applied bias changes the phase shift in the arm of the MZ interferometer, which is observed as a change in transmittance. The phase shift was extracted from the spectrum using the following equation: $\Delta\varphi = 2\pi\Delta\lambda/FSR$. The phase-shifter loss was estimated by comparing phase shifters of different lengths.

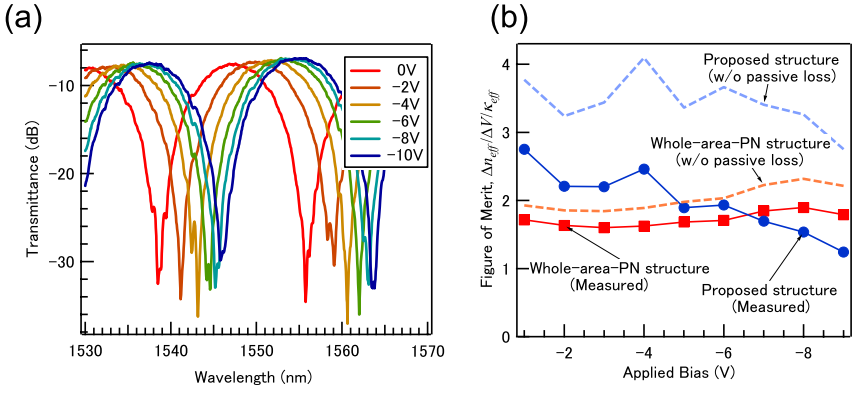

Fig. 4. (a) Transmittance of a MZ interferometer for various bias conditions, and (b) the measured $\Delta n_{eff}/\Delta V/\kappa_{eff}$ of the proposed structure and the whole-area-PN structure.

Fig. 4 (b) shows the FOMs ($\Delta n_{eff}/\Delta V/\kappa_{eff}$) estimated from the results above. The FOM of the proposed structure is higher than that of the whole-area-PN structure under most of the tested bias conditions. This means that the proposed structure can be used as a low-loss phase shifter. The measured κ_{eff} includes the effect not only of the carrier absorption but also

DOI: 10.1587/elex.10.20130552
Received July 15, 2013
Accepted August 02, 2013
Publicized August 15, 2013
Copyedited September 10, 2013

of the passive loss, such as loss caused by optical scattering due to surface roughness of the waveguides. The passive loss of the waveguide is considered to be 0.75 dB/cm from the measurements of the passive waveguide. If the passive loss did not exist, the FOM in each structure would be improved as the dotted line in the Fig. 4 (b). In comparison between the two structures, we find that the proposed structure has higher potential to decrease the phase shifter loss by further reduction of the passive loss.

3.3 Characterization of the Mach–Zehnder modulator with a 10-Gbps NRZ-OOK modulation

We fabricated a silicon MZM using the proposed phase shifter of 6-mm length in both arms, as shown in Fig. 5 (a). Channel waveguides are connected to the phase shifter, and a Y-junction is used as a branch of the MZ interferometer. For low-loss coupling to the fiber, inverted-taper type mode-field converters were fabricated on both edges of the waveguide. The electrode formed on the silicon waveguide is a coplanar traveling-wave electrode to achieve impedance matching, which is made of aluminum. The two arms of the MZM are each covered by a GSG transmission line.

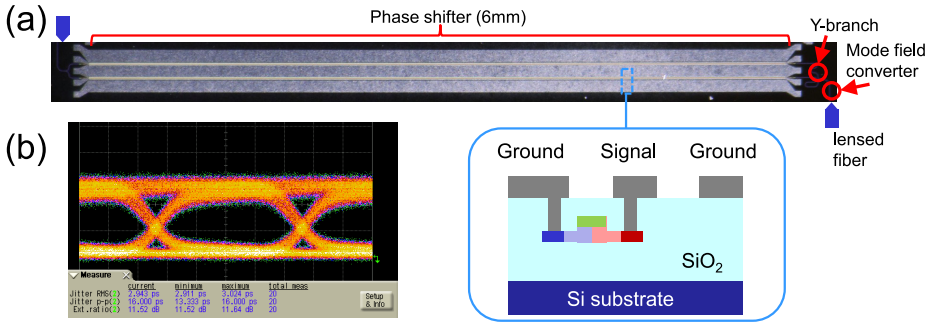

Fig. 5. (a) Fabricated silicon MZ modulator and (b) eye-diagram at 10 Gbps NRZ-OOK operation.

The fiber-to-fiber loss of the MZM is 9 dB for optical wavelengths in the C- and L-bands. The loss of the 6-mm phase shifter is estimated to be 1.6 dB at 1550 nm from the propagation loss of the proposed phase shifter, 2.7 dB/cm. The other main losses are the fiber coupling loss of 2.5 dB/facet and the excess loss of 1 dB in each Y-junction for the splitter/combiner. Use of a lower loss fiber coupler [15] and a splitter/combiner based on multi-mode interferometer (MMI) [16] will reduce the fiber-to-fiber loss to about 6 dB.

Using the fabricated MZM, we demonstrate a 10-Gbps NRZ-OOK modulation. Operating conditions are as follows: push-pull operation with 6 V_{pp}, 4 V DC offset bias in each arm, and 1549.4 nm input wavelength. The $V_\pi L_\pi$ of the phase shifter is 7.2 V·cm. The eye-diagram shown in Fig. 5 (b) shows a clear eye-opening with an extinction ratio (ER) of more than 11 dB at 10 Gbps. Thus, the fabricated MZM realizes both a phase-shifter loss as low as 1.6 dB and a high-speed operation with an ER of 11 dB at 10 Gbps.

The $V_\pi L_\pi$ of the proposed structure is larger than the 3 V·cm value for the whole-area-PN structure. This large $V_\pi L_\pi$ requires a longer phase shifter. However, the 7-mm silicon MZM including the 6-mm phase shifter is much shorter than lithium niobate MZMs. Another concern is the effects on

DOI: 10.1587/elex.10.20130552
Received July 15, 2013
Accepted August 02, 2013
Publicized August 15, 2013
Copyedited September 10, 2013

the high-speed response. The electrical loss of the phase shifter is 1.0 dB/mm at 5 GHz (fundamental frequency of 10 Gbps), which reduces the bandwidth of the MZM. The velocity mismatch of the electrical and optical signals also reduces the bandwidth. The improvement to the traveling-wave electrodes using techniques, such as velocity matching as reported in [4, 17, 18], is expected to help in realizing a higher bitrate of modulation.

4 Conclusion

We proposed a phase shifter with a bottom PN junction formed by restricted-depth doping for use in silicon MZMs. The simulations and experiments showed that the proposed structure has a high FOM ($\Delta n_{eff}/\Delta V/\kappa_{eff}$) and can be used as a low-loss phase shifter. The fabricated silicon MZM of 6-mm length had a low phase-shifter loss of 1.6 dB. The modulation with a 10-Gbps NRZ-OOK with an ER of 11 dB was demonstrated using the MZM with a 6 V_{pp} driving voltage on each arm. The fiber-to-fiber loss of the fabricated device was 9 dB. Combining the proposed phase shifter with lower loss passive components, such as an MMI-type branch and an improved mode-field converter, will reduce the insertion loss of the MZM to as low as that of LN MZMs. Thus, the silicon MZM with the proposed phase shifter is a good candidate for use as a low-loss modulator for long-haul telecommunication systems.

DOI: 10.1587/elex.10.20130552
Received July 15, 2013
Accepted August 02, 2013
Publicized August 15, 2013
Copyedited September 10, 2013